Volume 5, Issue 3, pp. 41-46, 2021.
International Journal of Scientific Engineering and Science
ISSN (Online): 2456-7361

Heterojunction Photovoltaic Systems with Plasmon Enhanced Efficiency

A. Axelevitch[1], I. Vokhgeit[1], M. Shatalov[2]
[1]Engineering Faculty, Holon Institute of Technology (HIT), Holon 5810201, Israel
[2]Chemical Engineering Department, Ariel University, Ariel 4070001, Israel

***Abstract*— Improving the efficiency of photovoltaic cells is one of the main directions of today's energy challenge. One of the encouraging methods for this is the use of the generation of plasmons in a photovoltaic structure under the influence of solar radiation. For this purpose, metal nanostructures can be used embedded in a semiconductor p-n junction of a photovoltaic cell. In this work, we investigated the heterojunction semiconductor structure of ZnO:Al grown the single-crystalline Si surface. To create the plasmon effect, the nanosized island thin Au film was placed between the semiconductors. All thin films used in the system were grown by the magnetron sputtering method. To compare the effect of the gold interlayer on the properties of solar cells, two series of samples were prepared simultaneously with one difference - a thin gold layer in some of the samples. The measured generated current and voltage are significantly increased compared to the same structure without a gold interlayer, about 10 times. In this work, we present an experimental confirmation of the increase in the efficiency of photoelectric conversion due to the generation of plasmons in gold nanoislands. Nanosized gold islands produce additional resonant electrons when exposed to sunlight and inject them into the conductive zone of the emitter layer. Thus, the efficiency of the photovoltaic cells is greatly increased.*

***Keywords*— Al doped Zinc Oxide, Gold island films, Localized surface plasmon-polariton, Solar cells.*

I. INTRODUCTION

Indium-tin oxide (ITO) thin films deposited on the silicon surface can form a rectifying electrical junction that enables to prepare effective photovoltaic (PV) constructions [1-3]. It was shown that the solar cells of such type can reach a value above 10% efficiency [4]. ITO is currently the highly popular transparent conductive coating (TCO), however this material is relatively expensive and rare [5]. So, searches for alternative materials become actual at the last time.

One of promising materials which was applied for fabrication a heterojunction with silicon is the aluminium doped zinc oxide (AZO) [5,6]. ZnO is a unique material. It is a wide-band semiconductor of class A_2B_6 with a straight-bandgap of width 3.4 eV, transparent in the visible range and sufficiently conductive to replace films of tin and indium oxides in various applications [7-9]. It is interesting that ZnO may be used as a dielectric barrier layer and as a transparent conductive layer when it doped by such materials as Al, Ga, In, Sn, N_2, Cd.

ZnO thin films may be prepared by various methods: by heating of thin metal Zn films in the air environment [10], by electrochemical deposition [11], by growth from the gas phase through the liquid phase (VLS-method) [12], by thermal evaporation in vacuum with thermal decomposition from gas phase [13], by hydro-thermal method [14], by growth from a gel-phase [15], by magnetron sputtering [16-18]. We used the magnetron co-sputtering method to prepare AZO films because of its simplicity and the possibility of precise control of the composition of the grown films by varying the sputtering power for different sources.

Theoretical calculation of possible conversion efficiency in the heterojunction PV cells based on the semiconductor junction between n-type ZnO and monocrystalline Si of p-type shows that this value can reach 20.3% [19]. However, experimental measurements present lower results of 2.82% [20] or 3.64% [21]. One of ways to improve the solar cells performance is to introduce the metal nanoparticles in the p-n junction. Introduction of palladium nanoparticles into the silicon pn-junction results in the conversion efficiency doubling [22]. The similar effect was revealed with use the gold nanoparticles [23]. Moreover, introducing the gold nanoparticles in the ITO/p-Si heterojunction shows significant increasing of the conversion efficiency [24]. Authors of mentioned above researches [22-24] explain their results by appearing a localized surface plasmon resonance (LSPR) in the low-dimensional metal islands undergo light irradiation. If these islands form the Schottky contacts with the semiconductor and each nano-diode is in the forward biased electrical field, electrons that appeared due to LSPR inject into conductive band of the semiconductor and increase by this way an amount of useful electricity [25].

One approach to build cheaper and more efficient PV structures is to use heterostructures instead of pn-junctions built from a single material. Thus, processes such as ion implantation or diffusion can be excluded from the technological chain. Therefore, in photovoltaic structures based on the use of p-type silicon wafers, an n-type silicon emitter, prepared by ion implantation, diffusion or atomic layer epitaxy, may be replaced by another semiconductor layer with a certain electron's concentration. Typical examples for such structures are n-ZnS/p-Si and n-ZnS:Al/p-Si heterojunction [26], or ITO/A-SI:H/SI heterostructure [3]. Here, the ITO (In2O3-SnO2) layer was used as an emitter on the PV heterostructure. The aim of this work is to study the possibility of increasing the efficiency of the structure of a photoelectric heterojunction using a thin island metal film embedded in a p-n junction. Here we present the results of our experimental tests.

II. Experimental Details

All experiments on thin films deposition were carried out in a VST service RF-DC sputtering system, model TESF-842, equipped with a turbomolecular pump enabling a residual pressure lower than 5×10^{-7} Torr [27]. The system includes three magnetrons of 2 inch in diameter and enables the simultaneous co-sputtering process using a 13.56 MHz, 300 W RF generator and two DC supplies of 1000 W each one. All thin films were deposited at argon atmosphere with the pressure of 3-5 mTorr.

ZnO thin films were deposited from pure ZnO target as using the RF supply as the DC supply. Thin films of ZnO doped by Al were deposited simultaneously from two targets. Here, the RF power was supplied the ZnO target and the DC power was applied to the Al target. Also, we tried deposit these films with application of DC power to the ZnO target and RF power to the Al. These thin films were grown at room temperature and they were annealed after deposition in vacuum at 300, 400 and 500^0C through one hour. Amount of aluminium in the ZnO matrix was controlled by a relation of power applied to the Al target. The slide-glasses were used as substrates in all experiments. In the experiments, we varied the sputtering power applied to the targets, annealing temperature and the aluminum concentration in the growing films.

Gold island thin films and aluminium upper and rear electrodes were also prepared using the same sputtering machine. The photovoltaic structures were prepared on the (100) surface of the single-crystalline p-type silicon substrates with resistivity of ~5-9 Ω·cm. The glass slides were applied as witness substrates to measure and study the optical properties of grown thin films. Each deposition of metal and ZnO:Al thin films was provided on both silicon and glass substrates. Figure 1 represents a side view of the grown thin film structure. We used the gold island thin films to produce the localized surface plasmon resonance under light irradiation.

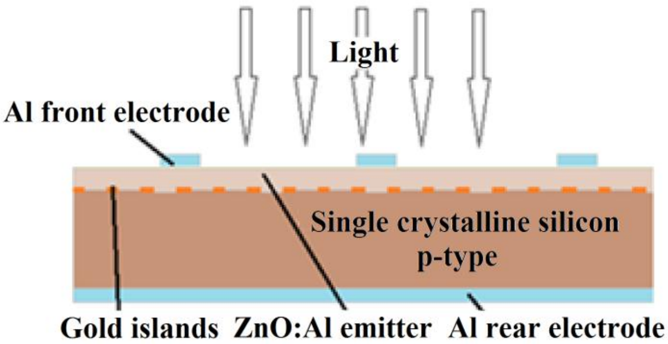

Fig. 1. Experimental PV structure.

External view of the prepared samples is shown in figure 2. The sample represents a multilayer system grown on the single-crystalline substrate of p-type. The front surface of the substrate is coated in series by gold island interlayer with approximate thickness of 2 nm and transparent conductive oxide ZnO:Al (TCO) thin film performing the emitter functions. Optical properties of the films were measured using the spectrophotometer UV-VIS "BioMate 3S" at the wavelength 200-1100 nm. The films topography was studied using the metallurgical microscope Hirox RH-2000. The surface resistivity was measured by the standard four-point method using the Macor-probe of MDC. Approximate estimation of the films thickness was carried out by weighing of the substrates before and after deposition using the analytical balance ASB-220-C2. Dynamical Hot-Probe method [28] was used for characterization of the concentration and mobility of the major charge carriers of grown ZnO:Al thin films and the Si substrates.

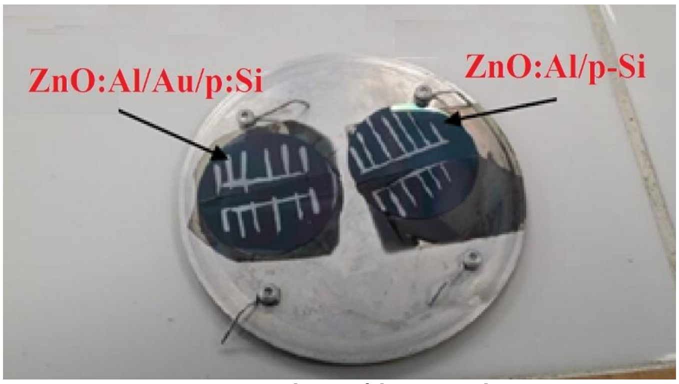

Fig. 2. External view of the PV samples.

The XRD measurements of the sputtered samples were carried out with a PANalytical X'Pert Pro (Malvern Panalytical Ltd., UK) diffractometer with $Cu_{K\alpha}$ source. Magnified, high resolution images of the deposited ZnO and Al:ZnO films were obtained with scanning electron microscopy (SEM) using a TESCAN MAIA3 device (Czech Republic). Surface topography of the gold thin films was observed using the SPM D1300 in AFM contact mode.

In order to compare the influence of gold islands imbedded into the semiconductor junction of PV cell on their parameters, we prepared a series of the same pairs of samples. In the pair, one of the samples was prepared with gold island film, and the second one was built without a metal interlayer. All the rest of parameters of the samples remained the same. To obtain the I-V and P-V characteristics of our PV-structures, they were measured at the same conditions at constant temperature of 20^0C under illumination of the solar light simulator (Solar Simulator, ABET Technologies, USA) providing on the distance 5 cm the maximum light intensity of ~38500 Lx that relates to approximately 1280 W/m^2.

III. Results and Discussion

A. Structure and topology of deposited thin films

Figure 3 represents the XRD pattern of the ZnO film deposited through 30 min on the glass substrate.

Analysis of XRD profile indicates that ZnO thin films have a polycrystalline wurtzite crystal structure with preferential growth of crystallites along [002] orientation (c-axis). There were no registered zincblende phase inclusions in ZnO films. The average crystallite size calculated from XRD pattern according to *the well-known* Scherrer equation was about 10 nm. This result is in well agreement with the SEM images presented in the inset in fig. 4.

International Journal of Scientific Engineering and Science
Volume 5, Issue 3, pp. 41-46, 2021. ISSN (Online): 2456-7361

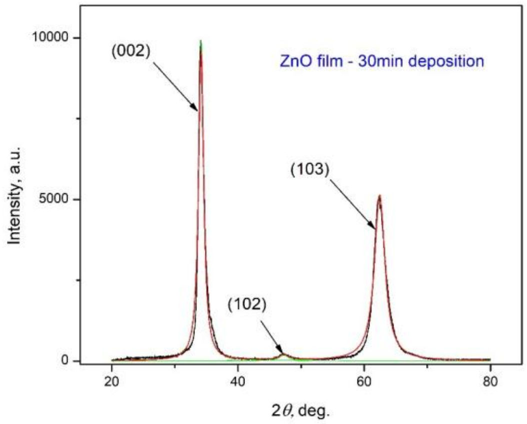

Fig. 3. XRD pattern of the ZnO thin film.

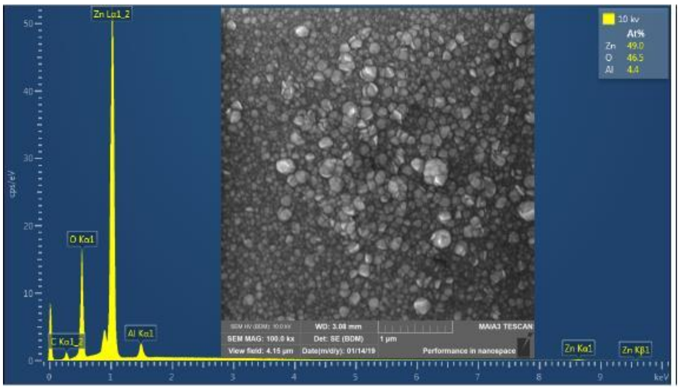

Fig. 4. EDS spectrum of ZnO:Al thin film. Inset presents the SEM image of the film.

The thin gold films were non-continuous and they were consisted of disks with diameter of 12-14 nm and height of 2-3 nm. Their sheet resistance is sufficiently high. These films were embedded into the p-n junction formed by ZnO:Al thin film deposited on the silicon surface. Figure 5 represents the AFM 3D topography of thin island gold film with thickness of 2-3 nm. This film consists of islands regularly distributed on the substrate surface and contains approximately 30 islands on the area of 100×100 nm^2.

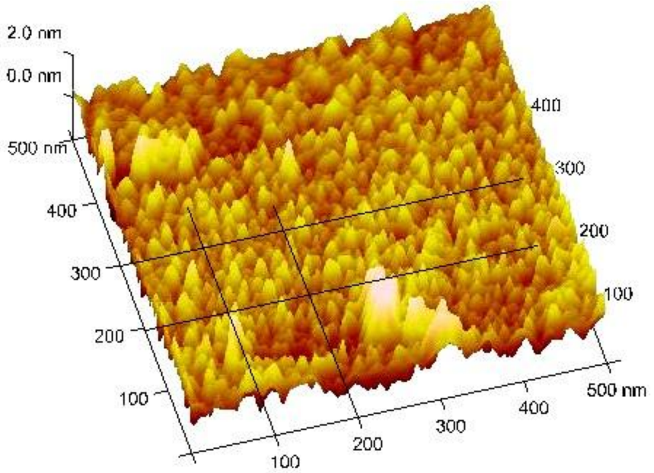

Fig. 5. AFM image of the gold film of 2 nm thick on the glass substrate.

B. Optical properties of deposited thin films

Figure 6 represents the transmittance spectra recorded for thin gold film and for ZnO:Al film. Also, the spectrum of pure glass substrate presented here.

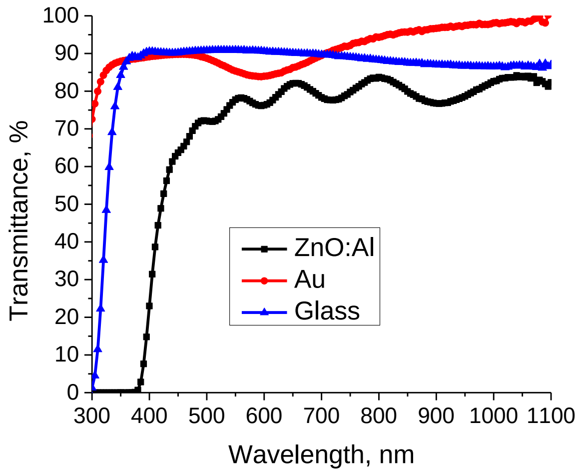

Fig. 6. Transmittance spectra of thin films deposited on the silicon substrate.

As shown, gold island films deposited during short time represent the large absorption peaks situated through visible part of spectrum. These peaks characterize arising the plasmon behaviour of electrons in the thin metal islands. The thicker films deposited by this method not show such absorption peak since the localized plasmon-polaritons disappear in the coalescing films [29]. Deepness, largeness and location of absorption peaks fully defined by the material of metal, and shape and dimensions of islands.

A bandgap of Al doped ZnO film may be defined using the transmittance characteristic (see fig. 6) by the well-known method in the high absorption region [30]. The graphical solution is presented in fig. 7.

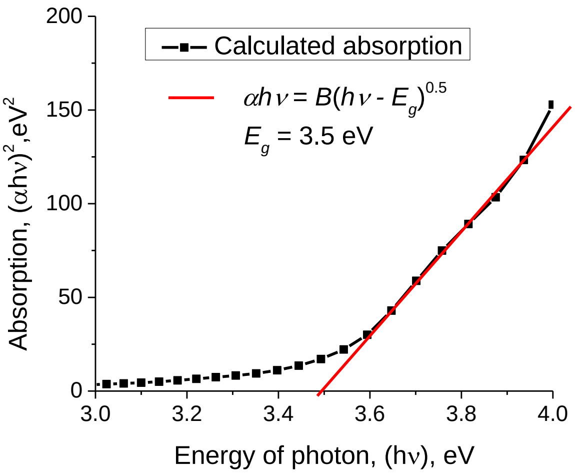

Fig. 7. Graphical calculation of the bandgap.

C. Electrical properties of deposited thin films

Electrical properties of silicon substrates and deposited thin films were evaluated using the dynamical Hot-Probe

International Journal of Scientific Engineering and Science
Volume 5, Issue 3, pp. 41-46, 2021. ISSN (Online): 2456-7361

method and the conventional four-probe method. The island gold films have presented very high sheet resistance. Figure 8 presents the hot-probe characteristics measured for silicon substrates.

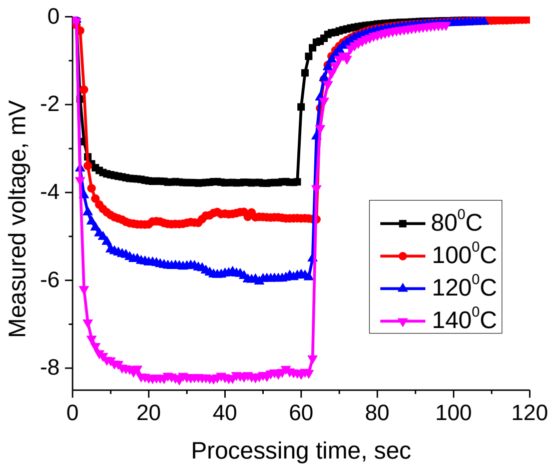

Fig. 8. Hot-probe characteristics of Si substrates.

According to measured characteristics presented on fig. 8 and known resistivity, the Si substrates are single-crystalline silicon of p-type containing p = $2 \cdot 10^{15}$ cm^{-3} major charge carriers.

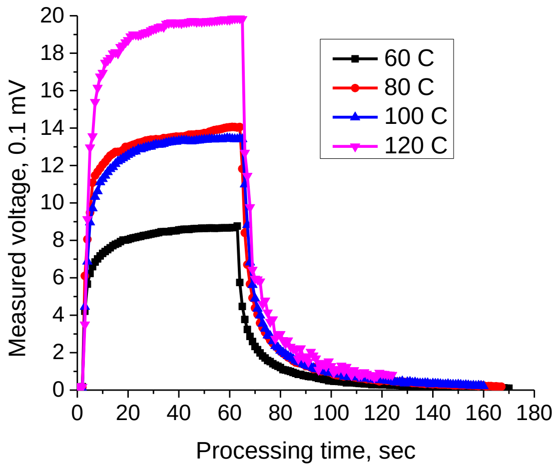

Fig. 9. Hot-probe characteristics of the Al:ZnO film.

ZnO:Al thin films represent n-type semiconductor layers (see fig. 9) with measured sheet resistance of ~ 18 Ω/sq. Calculation of major charge carriers results in approximately $9 \cdot 10^{15}$ cm^{-3} and mobility of ~15 cm^2/V·s.

D. Photovoltaic response of grown structures

The I-V characteristics were measured using a variable load resistor. The load resistance was varied in the interval from 0 up to 2500 Ω. Figure 10 present I-V characteristics measured for samples with two different structures: (a) Al/ZnO:Al/Si/Al and (b) Al/ZnO:Al/Au/Si/Al. The P-V characteristics were calculated on the base of measured I-V characteristics.

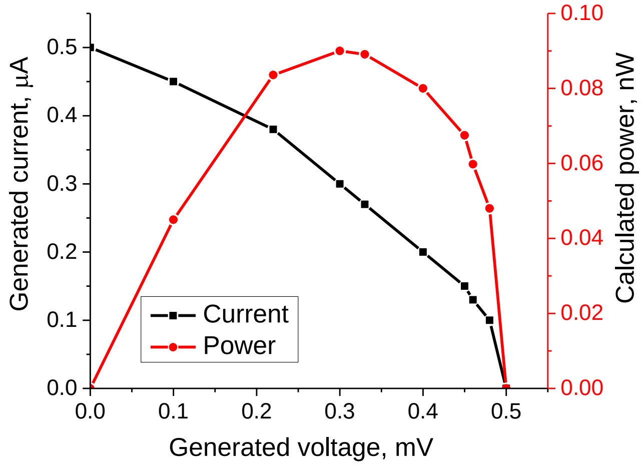

Fig. 10-a. I-V and PV characteristics of the Al/ZnO:Al/Si/Al photovoltaic structure.

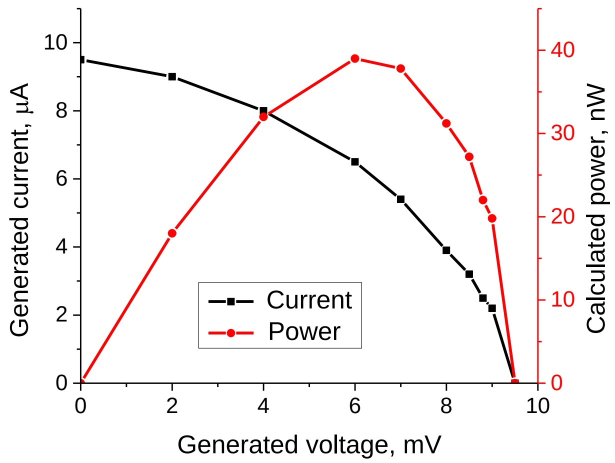

Fig. 10-b. I-V and PV characteristics of the Al/ZnO:Al/Au/Si/Al photovoltaic structure.

As shown in fig. 10-a and 10-b, the generated power in the structure with embedded gold interlayer is more than 10 times more than in the structure without it. In the samples with gold interlayer, the metal islands form different types of contact with emitter and base of the P/N structure.

As known, the type of contact depends on the type of semiconductor, P or N, and the difference between the work functions between contacting materials [31]. The work function of the gold is higher than the work function of the ZnO:Al. Therefore, the gold islands create Schottky contacts with the emitter and Ohmic contacts with the base of the diode P/N structure. At the same time, a natural high-strength electrical field is built-in in this P/N junction and our Schottky nano-diodes are undergo high electrical field. On the other hand, a light irradiation of the grown thin-film gold islands generates localized SPR inside the gold particles in the visible range of light. Under the built-in electrical field, the directly biased nano-diodes Schottky emit their excited additional electrons in the conducting band and the holes in the valence

Volume 5, Issue 3, pp. 41-46, 2021.
International Journal of Scientific Engineering and Science
ISSN (Online): 2456-7361

band of the P/N structure.

We illustrate this increasing by using the schematic energy band diagram. To create this diagram, we used parameters of applied materials shown in the table 1. Here are the reference data and our measured and calculated results.

TABLE I. Reference data for calculation.

Parameter	p-Si	Au	ZnO:Al	Source
Work function, φ, eV		5.47		[32]
Mobility, μ, $cm^2/V{\cdot}s$	410		50	[33] [34]
Bandgap, Eg, eV	1.12		3.5	[33] *
Relative permittivity, ε_r	11.9		3.66	[33] [34]
Electron affinity, χ, eV	4.05		4.5	[15] [19]
Film thickness, d, nm		~2	~800	*
Resistivity, Ω·cm	5-9			
Sheet resistance, Ω/sq		1.25M	18	*
Charge carrier concentration, n/p, cm^{-3}	$2{\cdot}10^{15}$	$5.9{\cdot}10^{22}$	$9{\cdot}10^{15}$	**

* Our measurements;

** Calculation, $n = \frac{1}{q\mu\rho}, cm^{-3}$;

Figure 11 represents the schematic energy diagram built using electrical and optical properties of deposited gold and ZnO:Al thin films. Calculations of a built-in potential and bands bending were provided according to Anderson' rule [19,26].

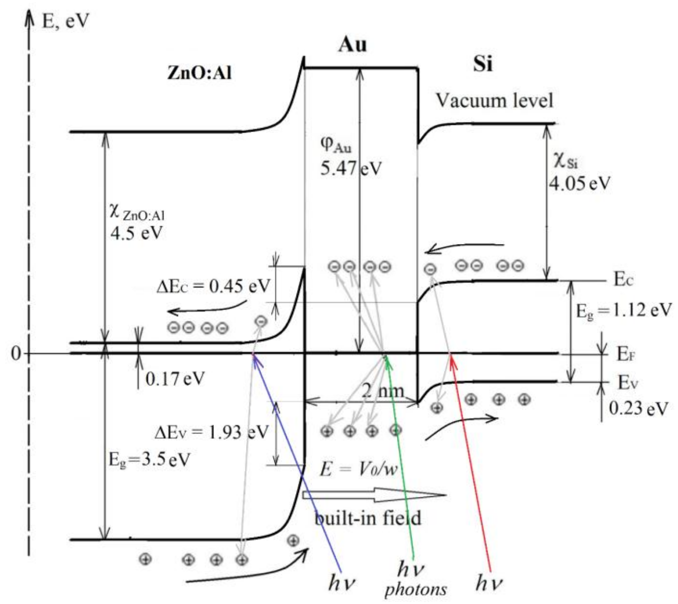

Fig. 11. A schematic energy diagram for the experimental PV cell with embedded gold islands.

This diagram illustrates the behaviour of p-n heterojunction with embedded gold island film under illumination. As it was mentioned above, the gold particle with a work function greater than the work function of the emitter ZnO:Al layer of n-type and greater than that of p-type base crystalline Si is embedded inside the depletion region with width w. This width is a sum of depletion regions in the TCO-Au contact and in the Au-Si contact: $w = w_{Si} + w_{TCO}$. Therefore, it forms a Schottky contact with the emitter TCO layer and an Ohmic contact with the base (p-type silicon). This particle is subjected to a strong electric field $E = V_b/w$ produced by the built-in potential, V_b, in the depletion region. Thus, all the gold particles form a set of forward-biased nano-diodes Schottky.

Under solar light irradiation, *hv*, we seeing two mechanisms of absorption: first one is a usual absorption of the photon in the active part of the solar cell producing one pair electron-hole, second mechanism is an absorption by the gold particle producing LSPR in gold particles. Excited electrons from the gold islands are injected into the conducting band of the semiconductor due to the resonance energy exceeding the Schottky barrier. These additional electrons are collected by the emitter electrode, thus increase the load current. So, each photon absorbed by the gold particle produces a lot of charged carriers due to polarization of the gold and emit them into the conductive (electrons) and valence (holes) bands of the joined semiconductors. Therefore, we obtain the amplification effect or the photon amplifier generating additional charged carriers utilized in the grown structure. Parallel connection of a plurality of nano-diodes Schottky to the silicon p-n junction leads to increase in the voltage generated by the system. Using the additional charged carriers generated within the gold particles and injected into the semiconductor environment, we can increase the useful electricity.

IV. Conclusions

In this paper, we experimentally investigated the effect of island gold films embedded into the P/N junction on the properties of PV structures. It was shown that non-continuous gold thin films deposited using magnetron sputtering appear the localized surface plasmon resonance behavior under illumination at light of visible spectrum. The gold island films embedded into the ZnO:Al/Si heterojunction have appeared significant increase in the PV cell efficiency.

References

[1] E.V. Monakhov, R. Balasundaraprabhu, N. Muthukumarasamy, B.G. Svensson, Electronic properties of the interface between Si and sputter deposited indium-tin oxide, *Materials Science and Engineering* B 159-160 (2009) 314-317.

[2] M. Huang, Z. Hameiri, A.G. Alberle, T. Mueller, high electron mobility indium tin oxide films for heterojunction silicon wafer solar cell applications, *The 6th World Conference on Photovoltaic Energy Conversion*, (2014) 655-656, https://www.researchgate.net/publication/275037739

[3] A.G. Uliyashin, K. Maknys, J. Christensen, A.Yu. Kuznetsov, B.G. Svensson, Properties of thin emitter of ITO/A-Si:H/Si heterojunction solar cells, *20th European Photovoltaic Solar Energy Conference*, 6-10 June 2005, Barselona, Spain, 1078-1081.

[4] V. Vasu, A. Subrahmanyam, Carrier transport mechanism in indium tin oxide (ITO)/silicon heterojunctions: effect of chlorine, *Appl. Phys.* A 80 (2005) 823-827.

[5] N. Neves, AZO – The replacement for ITO?, *Ceramic Applications* 3/1 (2015) 62-66.

[6] R. Romero, M.C. Lopez, D. Leinen, F. Martin, J.R. Ramos-Barrado, Electrical properties of the n-ZnO/c-Si heterojunction prepared by

chemical spray pyrolysis, *Materials Science and Engineering* B 110 (2004) 87-93.

[7] K. Ellmer, A. Klein, B. Rech, *Transparent Conductive Zinc Oxide*, Springer, Berlin 2007.

[8] S.B. Qadri, H. Kim, H.R. Khan, A. Pique, J.S. Horwitz, D. Chrisey, W.J. Kim, E.F. Skelton, “Transparent conducting films of In_2O_3-ZrO_2, SnO_2-ZrO_2 and ZnO-ZrO_2”, *Thin Solid Films* 377-378 (2000) 750-754.

[9] K. Lovchinov, M. Ganchev, M. Petrov, H. Nichev, D. Dimova-Malinovska, J.S. Graff, A. Ulyashin, “Electrochemically deposited nanostructured ZnO layers on the front side of c-Si solar cell”, *Bulgarian Chemical Communications*, 45/A (2013) 153-158.

[10] N. Parkansky, G. Shalev, B. Alterkop, S. Goldsmith, R.L. Boxman, Z. Barkay, L. Glikman, H. Wulff, M. Quaas, Growth of ZnO nanorods by air annealing of ZnO films with an applied electric field, *Surf. Coa. Tech*. 201 (2006) 2844–2848.

[11] K. Lovchinov, M. Ganchev, M. Petrov, H. Nichev, D. Dimova-Malinovska, J. S. Graff, Al. Ulyashin, Electrochemically deposited nanostructured ZnO layers on the front side of c-Si solar cell, *Bulg. Chem. Commun*., 45/A (2013) 153–158.

[12] H. Qi, E.R. Glaser, J.D. Caldwell, and S.M. Prokes, Growth of Vertically Aligned ZnO Nanowire Arrays Using Bilayered Metal Catalysts, *J. Nanomater*. (2012) ID 260687, 7 pages, doi:10.1155/2012/260687.

[13] E. Muchuweni, T.S. Sathiaraj, H. Nyakotyo, Synthesis and characterization of zinc oxide thin films for optoelectronic applications, *Helyion* 3 (2017) e00285.

[14] C. Opoku, A.S. Dahiya, C. Oshman, F. Cayrel, G. Poulin-Vittrant, D. Alquier, N. Camara, Fabrication of ZnO Nanowire Based Piezoelectric Generators and Related Structures, *Physics Procedia* 70 (2015) 858 – 862.

[15] G. Kiriakidis, I. Kortidis, S.D. Cronin, N.J. Morris, D.R. Cairns, K.A. Sierros, Tribological investigation of piezoelectric ZnO films for rolling contact-based energy harvesting and sensing applications, *Thin Solid Films* 555 (2014) 68-75.

[16] M. Lv, X. Xiu, Z. Pang, Y. Dai, S. Han, Transparent conducting zirconium-doped zinc oxide films prepared by rf magnetron sputtering, *Appl. Surf. Sci*. 252 (2005) 2006-2011.

[17] M. Lv, X. Xiu, Z. Pang, Y. Dai, L. Ye, C. Cheng, S. Han, Structural, electrical and optical properties of zirconium-doped zinc oxide films prepared by radio frequency magnetron sputtering, *Thin Solid Films* 516 (2008) 2017-2021.

[18] H.F. Zhang, C.X. Lei, H.F. Liu, C.K. Yuan, Low-temperature deposition of transparent conducting ZnO:Zr films on PET substrates by DC magnetron sputtering, *Appl. Surf. Sci*. 255 (2009) 6054-6056.

[19] B. Hussain, A. Aslam, T.M. Khan, M. Creighton, B. Zohuri, Electron Affinity and Bandgap Optimization of Zinc Oxide for Improved Performance of ZnO/Si Heterojunction Solar Cell Using PC1D Simulations, *Electronics* 8 (2019) 238-(1-8).

[20] L. Chen, X. Chen, Y. Liu, Y. Zhao, X. Xhang, Research on ZnO/Si heterojunction solar cells, *J. of Semiconductors* 38/5 (2017) 054005-(1-11).

[21] K.H. Abass, M.K. Mohammed, Fabrication of ZnO:Al/Si Solar Cell and Enhancement its Efficiency Via Al-Doping, *Nano Biomedicine and Engineering* 2019-2020.

[22] M. Atyaoui, A. Atyaoui, m. Khalifa, J. Elyagoubi, W. Dimassi, H. Ezzaouia, Enhancement in photovoltaic properties of silicon solar cells by surface plasmon effect of palladium nanoparticles, *Superlattice and Microstructures* 92 (2016) 217-223.

[23] A. Axelevitch, B. Gorenstein, G. Golan, Application of gold nano-particles for silicon solar cells efficiency increase, *Appl. Surf. Sci*. No.315, 2014, pp. 523-526.

[24] A. Axelevitch, Application of Embedded Metal Nanoparticles for Solar Cells, *Int. Journal of Renewable Energy Sources* 1 (2016) 32-37.

[25] A. Axelevitch, G. Golan, Solar cells efficiency increase using thin metal island film, *J. of Solar Energy*, 2013 (2013), Article ID 478219, 5 pages.

[26] E.M. Nasir, Fabrication and Characterization of n-ZnS/p-Si and n-ZnS:Al/p-Si Heterojunction, *International Journal of Engineering and Advanced Technology (IJEAT)*, Vol.3, No.2, 2013, 425-429.

[27] O. Briot, M. Moret, C. Barbier, A. Tiberj, H. Peyre, A. Sagna, S. Contreras, Optimization of the properties of the molybdenum back contact deposited by radiofrequency sputtering for $Cu(In_{1-x}Ga_x)Se_2$ solar cells, *Solar Energy Materials and Solar Cells* 174 (2018) 418-422.

[28] A. Axelevitch, G. Golan, "Hot-probe method for evaluation of majority charged carriers concentration in semiconductor thin films", *Facta Universitatis: Series Electronics and Energetics* 27/3, (2013) 187-195.

[29] A. Axelevitch, B. Apter, In-situ investigation of optical transmittance in metal thin films, *Thin Solid Films* 591 (2015) 261-266.

[30] M. Fox, *Optical properties of Solids*, Oxford, University Press, 2010.

[31] B. Van Zeghbroek, *Principles of Semiconductor Devices*, 2011, http://ece-www.colorado.edu/~bart/book/

[32] *Electron work function of the elements*, 1979, http://public.wsu.edu/~pchemlab/documents/Work-functionvalues.pdf

[33] A. Goetzberger, J. Knobloch, B. Voss, *Crystalline Silicon Solar Cells*, John Wiley & Sons, 1998.

[34] V. Quemener, Electrical Characterization of Bulk and Thin Film Zinc Oxide, PhD thesis, University of Oslo, 2012.